

MICROCAVITÉS ET CRISTAUX PHOTONIQUES

MICROCAVITIES AND PHOTONIC CRYSTALS

Quantum optical effects in semiconductor microcavities

Elisabeth Giacobino, Jean-Philippe Karr, Gaëtan Messin, Hichem Eleuch, Augustin Baas

Laboratoire Kastler Brossel, université Pierre et Marie Curie, École normale supérieure et CNRS, case 74, 4, place Jussieu, 75252 Paris cedex 05, France

Received and accepted 6 December 2001

Note presented by Guy Laval.

Abstract

Investigations of quantum effects in semiconductor quantum-well microcavities interacting with laser light in the strong-coupling regime are presented. Modifications of quantum fluctuations of the outgoing light are expected due to the non-linearity originating from coherent exciton–exciton scattering. In the strong-coupling regime, this scattering translates into a four-wave mixing interaction between the mixed exciton–photon states, the polaritons. Squeezing and giant amplification of the polariton field and of the outgoing light field fluctuations are predicted. However, polariton–phonon scattering is shown to yield excess noise in the output field, which may destroy the non-classical effects. Experiments demonstrate evidence for giant amplification due to coherent four-wave mixing of polaritons. Noise reduction below the thermal noise level was also observed. To cite this article: E. Giacobino et al., C. R. Physique 3 (2002) 41–52. © 2002 Académie des sciences/Éditions scientifiques et médicales Elsevier SAS

semiconductor microcavities / strong coupling / squeezing / noise reduction / parametric amplification / four-wave mixing

Optique quantique dans les microcavités semi-conductrices

Résumé

Cet article présente les recherches sur les effets quantiques dans les microcavités semi-conductrices à puits quantiques interagissant avec un champ laser dans le régime de couplage fort. Les calculs montrent que les fluctuations quantiques du champ sortant doivent être modifiées à cause de la non-linéarité provenant de la diffusion cohérente entre excitons. En régime de couplage fort, cette interaction entre excitons se traduit en effet par un mélange à quatre ondes entre polaritons. Il en résulte une compression ou une amplification géante des fluctuations du champ de polaritons et du champ lumineux sortant. Cependant la diffusion phonon–polariton peut détruire les effets non classiques en ajoutant de l'excès de bruit aux fluctuations du champ sortant. Les expériences montrent l'amplification géante due au mélange à quatre ondes cohérent de polaritons. Une réduction du bruit au-dessous du niveau de bruit thermique a aussi été observée. Pour citer cet article: E. Giacobino et al., C. R. Physique 3 (2002) 41–52. © 2002 Académie des sciences/Éditions scientifiques et médicales Elsevier SAS

microcavités semi-conductrices / couplage fort / compression du bruit quantique / réduction du bruit / amplification paramétrique / mélange à quatre ondes

E-mail address: elisabeth.giacobino@spectro.jussieu.fr (E. Giacobino).

1. Introduction

In recent years, the optical properties of microcavities containing semiconductor quantum wells in the strong-coupling regime [1] have been the subject of detailed investigations [2]. However, quantum properties of the light reflected or emitted by microcavities containing semiconductor quantum wells have been much less studied. Quantum effects such as squeezing and antibunching of the outgoing light have been predicted and observed in microcavities containing atoms [3]. In semiconductor microcavities as in atomic ones, modifying the statistical properties of light requires a coherent non-linearity in the system. In addition, the non-classical features must not be destroyed by spurious fluctuations linked to the relaxation processes that are often more efficient in semiconductors than in atomic ensembles. In spite of numerous non-radiative relaxation processes that cause a fast decay of coherences, semiconductors have already been shown to exhibit coherent nonlinear effects [4], such as dynamical Stark shift [5]. Furthermore, recent experiments have demonstrated the possibility to modify the quantum fluctuations and to generate squeezing in semiconductors [6].

Several authors have presented theoretical studies of the quantum fluctuations of the light going out of a semiconductor microcavity containing one semiconductor quantum well [7–11]. The most realistic model assumes a non-linearity arising from exciton–exciton interaction [12]. In the strong-coupling regime, the process can be recast in terms of polaritons and can be interpreted as coherent polariton four-wave mixing [13]. For the non-linearity to be most efficient one requires energy and in-plane momentum conservation for the process where two pump polaritons (with momentum $k_{P\parallel}$) are converted into a signal polariton ($k_{\parallel} = 0$) and an idler polariton ($k_{\parallel} = 2k_{P\parallel}$). Due to the polariton specific dispersion shape, this is possible for a resonant pump at a specific ‘magic’ angle with a signal polariton at $k_{\parallel} = 0$. This configuration was used in several experiments [14–17], where a strong amplification was observed on the signal wave. An alternative configuration ensures the double energy and momentum resonance: it is the one where $k_{P\parallel} = 0$, with $k_{\text{signal}\parallel} = k_{\text{idler}\parallel} = 0$, the energy of the pump laser being resonant with the polariton energy at $k_{\parallel} = 0$. The coherence of the polariton four-wave mixing process was demonstrated in this regime [18].

For quantum optics, it is important to consider incoming fluctuations for the excitons that are not only zero-point vacuum fluctuations, but fluctuations related to the existing relaxation processes at non-zero temperature, as required by the fluctuation–dissipation theorem. This subject is a quite difficult one and can only be treated under strong approximations.

In a full quantum model, the polaritons are treated as a quantum field, having well defined amplitude and phase. The fluctuations on the various quadrature components of the polariton field may depend on the considered quadrature. The main predictions of such a model are the amplification of some quadrature components of the fluctuations of the polariton and of the associated outgoing light field and the deamplification of other quadratures. Under conditions in which the thermal noise is small enough, reduction of the fluctuations of the reflected light below the standard quantum noise is expected. The counterpart of the noise reduction on some quadrature components is a giant amplification in the fluctuations on other quadrature components, in particular on the amplitude, that has been observed experimentally [18]. It has the same physical origin as the non-linear amplification of the microcavity emission at the magic angle [14–17]. Deamplification of the emission below the level of thermal noise has been observed. However, squeezing below the standard quantum noise level has not been seen.

Engineering the quantum fluctuations of light in semiconductor materials would open the way to compact and highly integrable quantum devices, such as noiseless sources of light, thresholdless lasers or highly efficient all-optical switches. The possibility of using microcavities as memories for quantum information is also envisioned. The understanding of quantum properties of semiconductor microcavities is thus of great importance.

2. Model

The considered system is a microcavity containing a semiconductor quantum well embedded between two highly reflecting planar mirrors separated by a distance of the order of the wavelength. The discussion is limited to a two-band semiconductor. The electromagnetic field can excite an electron from the filled valence band to the conduction band, thereby creating a hole in the valence band. The electron–hole system possesses bound states, the excitonic states. We will only consider the lowest of these bound states, the 1s state.

Neglecting the spin degrees of freedom, we can write an effective interaction Hamiltonian for the coupled exciton–photon system in the cavity as [12,19,20]:

$$\begin{aligned}
 H = & \sum_k E_{\text{cav}}(k) \hat{a}_k^\dagger \hat{a}_k + \sum_K E_{\text{exc}}(K) \hat{b}_K^\dagger \hat{b}_K + \sum_k \frac{1}{2} \Omega_R (\hat{a}_k^\dagger \hat{b}_k + \hat{b}_k^\dagger \hat{a}_k) \\
 & + \sum_{K, K'} \sum_Q \hbar \alpha_{KK'Q} \hat{b}_K^\dagger \hat{b}_{K'}^\dagger \hat{b}_{K+Q} \hat{b}_{K'-Q} + \left(\sum_{K, K'} \sum_Q \hbar \alpha'_{KK'Q} \hat{b}_K^\dagger \hat{b}_{K'}^\dagger \hat{b}_{K+Q} \hat{a}_{K'-Q} + \text{H.C.} \right) \\
 & + \sum_{KK'} \beta_{KK'} \hat{b}_K^\dagger \hat{b}_{K'} (\hat{c}_{K-K'} + \hat{c}_{K'-K}^\dagger) + \left(\sum_{k j} \hbar \gamma_{kj} \hat{a}_k^\dagger \hat{A}_j + \text{H.C.} \right) \quad (1)
 \end{aligned}$$

The exciton and photon modes being quantized along the direction normal to the microcavity, we consider the lowest-order mode in this direction and the sums over k and K run for the momenta in the cavity plane only (the index in k_{\parallel} has been suppressed for simplicity). The first two terms correspond to the energies of the photons and of the excitons, where \hat{a}_k and \hat{b}_K are respectively the annihilation operators of a photon of in-plane momentum k and of an exciton of in-plane momentum K and $E_{\text{cav}}(k)$ and $E_{\text{exc}}(K)$ are the energies of the corresponding cavity and exciton modes. The third term corresponds to the exciton–photon coupling with a strength Ω_R , which is larger than the relaxation rates defined below, since we have assumed the strong-coupling regime. Due to the translational invariance in the plane of the semiconductor layers, excitons with a wave vector K in this plane can only be coupled with light having an equal in-plane wave vector $k = K$.

The fourth term describes the exciton–exciton scattering due to Coulomb interaction, while the fifth term represents the saturation of the photon–exciton interaction. These terms are at the origin of the nonlinear behaviour in the microcavity. The term before the last describes the exciton–phonon scattering, where \hat{c}_Q is the phonon annihilation operator. The last term represents the coupling between the electromagnetic field modes inside the cavity \hat{a}_k and outside the cavity \hat{A}_j , the latter being considered as a reservoir.

The linear part of the Hamiltonian given in equation (1) without the relaxation terms can be easily diagonalized for each k value using the polariton basis:

$$H_k = E_k^+ \hat{p}_k^{(+)\dagger} \hat{p}_k^{(+)} + E_k^- \hat{p}_k^{(-)\dagger} \hat{p}_k^{(-)} \quad (2)$$

where the energies of the upper $\hat{p}_k^{(+)}$ and lower $\hat{p}_k^{(-)}$ polaritons are written:

$$E_k^\pm = \frac{1}{2} \left(E_{\text{exc}}(k) + E_{\text{cav}}(k) \pm \sqrt{\delta_k^2 + \Omega_R^2} \right) \quad \text{with} \quad (3)$$

$$\delta_k = E_{\text{cav}}(k) - E_{\text{exc}}(k) \quad (4)$$

The polariton operators are given as functions of the photon and exciton operators as:

$$\hat{p}_k^{(-)} = -C_k \hat{a}_k + X_k \hat{b}_k, \quad \hat{p}_k^{(+)} = X_k \hat{a}_k + C_k \hat{b}_k \quad (5)$$

$$\text{with } X_k^2 = \frac{\delta_k + \sqrt{\delta_k^2 + \Omega_R^2}}{2\sqrt{\delta_k^2 + \Omega_R^2}} \quad (6)$$

$$\text{and } C_k^2 = \frac{\Omega_R^2}{2\sqrt{\delta_k^2 + \Omega_R^2}(\delta_k + \sqrt{\delta_k^2 + \Omega_R^2})} \quad (7)$$

The coefficients X_k^2 and C_k^2 represent respectively the exciton and photon fractions of the lower polariton, and the photon and exciton fractions of the upper polariton.

The coupling between the cavity electromagnetic modes and the reservoir of outside modes is a simple coupling between harmonic oscillators. It is well known [21–23] to lead to a relaxation of the cavity modes and to additional fluctuations in the resulting Heisenberg–Langevin equations. The corresponding terms are written:

$$\frac{d\hat{a}_k}{dt} = -\gamma_{ak}\hat{a}_k + \sqrt{2\gamma_{ak}}\hat{a}_k^{\text{in}} \quad (8)$$

where γ_{ak} is a relaxation rate that may be calculated from the γ_{kj} appearing in the Hamiltonian. In this equation, the fields inside the cavity are normalized in such a way that quantities such as $\langle \hat{a}_k^\dagger \hat{a}_k \rangle$ are numbers of particles, while the ‘incoming’ fields are such that $\langle \hat{a}_k^{\dagger \text{in}} \hat{a}_k^{\text{in}} \rangle$ is a number of particles per second.

The case of the relaxation of the excitons is much more intricate. The density is assumed to be low enough to neglect the relaxation due to direct exciton–exciton interaction, the fourth and fifth terms in the Hamiltonian yielding mainly coherent nonlinear interaction between the specific mode of interest and the pump mode directly excited by the outside field. At low density and low enough temperature, exciton relaxation mainly comes from the term before the last, through which an exciton mode \hat{b}_K is coupled to all the other exciton modes with a different wave number and to all the phonon modes fulfilling the condition of energy and wavevector conservation. In cavities in the strong coupling regime, the relaxation has been studied in detail by several authors [24–26]. However, the derivation of the corresponding fluctuation terms requires additional hypotheses, under which it can be shown that one can replace the exciton–phonon coupling Hamiltonian by a linear coupling to a single reservoir [27] with operators \hat{B}_j as:

$$H_{\text{rel}}^{\text{exc}} = \sum_{k,j} \hbar \beta_{kj} \hat{b}_k^\dagger \hat{B}_j + \text{H.C.} \quad (9)$$

Then, in the same way as for the photon field, the fluctuation–dissipation part in the Langevin equation for the excitons is written:

$$\frac{d\hat{b}_k}{dt} = -\gamma_{bk}\hat{b}_k + \sqrt{2\gamma_{bk}}\hat{b}_k^{\text{in}} \quad (10)$$

In the following, the treatment will focus on the case of only one photon mode irradiating the microcavity, with $k = 0$. Because of the in-plane momentum conservation in the exciton–photon interaction, this cavity mode is only coupled with one exciton mode of $K = 0$. The interaction between the exciton and the photon modes of interest can then be modeled by the coupling of two harmonic oscillators, together with an excitonic non-linearity coming from the terms in the second line of equation (1) with $K = K' = Q = 0$. The Hamiltonian of the coupled system can be written as:

$$H = E_{\text{cav}}\hat{a}^\dagger\hat{a} + E_{\text{exc}}\hat{b}^\dagger\hat{b} + \frac{\hbar}{2}\Omega_R(\hat{a}^\dagger\hat{b} + \hat{b}^\dagger\hat{a}) + \hbar\alpha\hat{b}^\dagger\hat{b}^\dagger\hat{b}\hat{b} + H_{\text{rel}} \quad (11)$$

with $E_{\text{cav}} = E_{\text{cav}}(0)$ and $E_{\text{exc}} = E_{\text{exc}}(0)$ and where the indices $k = 0$ have been left out. The nonlinear term describing saturation effects will not be treated here. It can be shown that it gives rise to small corrections

as compared to the previous one [28]. The term H_{rel} contains all the other terms of equation (1) discussed above.

The problem of the determination of the quantum optical properties of the outgoing field has some similarities with the one of a cavity containing atoms. The squeezing properties of the field going out of a cavity containing atoms in the strong-coupling regime were investigated in reference [29]. In order to compute the squeezing spectra of the output field of a microcavity containing excitons, one must take into account the fact that the non-linearity is different from the atomic one, and one has to include a thermal reservoir coupled to the exciton system.

The microcavity is irradiated by a coherent field from a laser of frequency ω_L . One mirror of the microcavity is perfectly reflecting, whereas the other one, having a small non-zero transmission coefficient, is the coupling mirror, through which the light is coupled in and out. Including relaxation processes, one derives from the Hamiltonian (11) evolution equations for the time-dependent electromagnetic field and exciton field operators inside the cavity:

$$\frac{d\hat{a}}{dt} = -(\gamma_a + i\delta_a)\hat{a} - ig\hat{b} + \sqrt{2\gamma_a}\hat{a}^{\text{in}} \quad (12)$$

$$\frac{d\hat{b}}{dt} = -(\gamma_b + i\delta_b)\hat{b} - ig\hat{a} - 2i\alpha\hat{b}^\dagger\hat{b}\hat{b} + \sqrt{2\gamma_b}\hat{b}^{\text{in}} \quad (13)$$

where γ_a and γ_b are the decay constants of the cavity field and of the exciton for $k = 0$, $\delta_a = E_{\text{cav}}/\hbar - \omega_L$ and $\delta_b = E_{\text{exc}}/\hbar - \omega_L$ are the detunings of the cavity and of the exciton from the frequency ω_L of the incoming laser field. The exciton to photon coupling constant is $g = \Omega_R/2\hbar$. The nonlinear coupling constant is α , which can be expressed as $2\alpha = 6e^2 a_{\text{exc}}/\hbar\epsilon A$, where a_{exc} is the Bohr radius of the exciton, ϵ is the dielectric constant of the quantum well, and A is the area of quantization. The fields \hat{a}^{in} and \hat{b}^{in} are the incoming electromagnetic and exciton fields, the characteristics of which will be discussed below.

In the input–output formalism [30], the output field is related to the intracavity and input fields by:

$$\hat{a}^{\text{out}} = \sqrt{2\gamma_a}\hat{a} - \hat{a}^{\text{in}} \quad (14)$$

This equation indicates that the outgoing field is the sum of the inside field transmitted through the coupling mirror and of the input field reflected by the mirror (the reflection coefficient has been replaced by 1 in this equation).

In equations (12) and (13), the fluctuating part of the terms $\sqrt{2\gamma_a}a^{\text{in}}$ and $\sqrt{2\gamma_b}b^{\text{in}}$ are the Langevin forces associated with the reservoirs for the electromagnetic field and for the excitons. The minimal values of these fluctuating terms correspond to the zero-point fluctuations (or vacuum fields) imposed by quantum mechanics. Additional fluctuations may arise from the specific scattering processes. Non-classical optical effects have been predicted by several authors in the case of vacuum incoming fluctuations [7–9]. When thermal fluctuation processes are included, squeezing of quantum fluctuations may disappear [10,11].

The incoming electromagnetic field is the laser coherent field, which is a classical field together with quantum fluctuations equal to the vacuum fluctuations. Thus the incoming field can be written as $\hat{a}^{\text{in}} = a^{\text{in}} + \delta\hat{a}^{\text{in}}$ where a^{in} is the classical mean value of the field and its fluctuations $\delta\hat{a}^{\text{in}}$ have a zero mean value. The only non-zero correlation function of the fluctuations is:

$$\langle \delta\hat{a}^{\text{in}}(t)\delta\hat{a}^{\text{in}\dagger}(t') \rangle = \delta(t - t') \quad (15)$$

The exciton field inside the cavity is coupled with a fluctuating field $\hat{b}^{\text{in}} = \delta\hat{b}^{\text{in}}$ that may have several contributions associated with the various relaxation processes. Here, as mentioned above, only the term coming from phonon scattering will be treated, as a coupling with a thermal bath [22,31]. The only two

non-zero correlation functions are then given by:

$$\langle \delta \widehat{b}^{\text{in}}(t) \delta \widehat{b}^{\text{in}\dagger}(t') \rangle = (1 + \langle n \rangle) \delta(t - t'), \quad \langle \delta \widehat{b}^{\text{in}\dagger}(t) \delta \widehat{b}^{\text{in}}(t') \rangle = \langle n \rangle \delta(t - t') \quad (16)$$

$\langle n \rangle$ is the mean number of excitations in the thermal bath, with $\langle n \rangle = 0$ at zero temperature $T = 0$.

To calculate the fluctuations of the outgoing light field, equations (2)–(3) are linearized in the vicinity of the operating point. To do so, the mean values of the fields have to be computed first.

3. Mean fields

In order to study the mean values of the electromagnetic and excitonic fields, equations (12) and (13) are rewritten for classical values of the field, removing the fluctuating terms, and solved in the steady state regime ($da/dt = db/dt = 0$). The equations are written:

$$(\gamma_a + i\delta_a)a + igb = \sqrt{2\gamma_a} a^{\text{in}} \quad (17)$$

$$(\gamma_b + i\delta_b)b + ig a^* b^2 \quad (18)$$

In the linear case ($\alpha = 0$), they yield simple analytical expressions for the mean photon numbers I_a and I_b of the fields:

$$\frac{I_a}{I^{\text{in}}} = \frac{2\gamma_a(\gamma_b^2 + \delta_b^2)}{(g^2 + \gamma_a\gamma_b - \delta_a\delta_b)^2 + (\gamma_a\delta_b + \gamma_b\delta_a)^2} \quad (19)$$

$$\frac{I_b}{I^{\text{in}}} = \frac{2\gamma_a g^2}{(g^2 + \gamma_a\gamma_b - \delta_a\delta_b)^2 + (\gamma_a\delta_b + \gamma_b\delta_a)^2} \quad (20)$$

where $I^{\text{in}} = |a^{\text{in}}|^2$ is the incoming laser field intensity. The intensity I^{out} of the reflected field:

$$a^{\text{out}} = \sqrt{2\gamma_a} a - a^{\text{in}} \quad (21)$$

is given by:

$$\frac{I^{\text{out}}}{I^{\text{in}}} = \frac{(g^2 - \gamma_a\gamma_b - \delta_a\delta_b)^2 + (\gamma_a\delta_b - \gamma_b\delta_a)^2}{(g^2 + \gamma_a\gamma_b - \delta_a\delta_b)^2 + (\gamma_a\delta_b + \gamma_b\delta_a)^2} \quad (22)$$

This enables one to calculate the reflectivity R and absorption $A = 1 - R$ of the microcavity. Absorption is found to be proportional to the excitonic field intensity:

$$\frac{I_b}{I^{\text{in}}} = \frac{A}{2\gamma_b} \quad (23)$$

Thus the absorption spectrum of the microcavity gives direct access to the variation of I_b with the laser frequency. When exciton and cavity are on resonance ($\delta_a = \delta_b$), the degeneracy is lifted due to the strong coupling, and the field intensities have two symmetrical peaks. The energy difference between the two peaks yields the vacuum Rabi splitting for the intracavity field, Δ_a , and for the absorption, Δ_b :

$$\Delta_a = 2\sqrt{g\sqrt{g^2 + 2\gamma_b(\gamma_a + \gamma_b)} - \gamma_b^2} \quad (24)$$

$$\Delta_b = 2\sqrt{g^2 - \frac{\gamma_a^2 + \gamma_b^2}{2}} \quad (25)$$

When non-linear processes are taken into account, there is no simple analytical expression for the field intensities. However, it is possible to write the incoming field intensity as a function of the excitonic field

intensity:

$$I^{\text{in}} = \frac{1}{2\gamma_a} \frac{(g^2 - \delta_a\delta_b + \gamma_a\gamma_b - \alpha\gamma_a I_b)^2 + (\gamma_a\delta_b + \gamma_b\delta_a - \delta_a\alpha I_b)^2}{g^2} I_b \quad (26)$$

This expression leads to bistability for high enough values of the non-linearity. Only preliminary observation of this effect has been obtained recently [27], in a situation where strong coupling is still present. Bistability observed in previous cases was due to the bleaching of the oscillator strength, causing the strong-coupling effect to disappear [33,34].

4. Predicted quantum fluctuations and squeezing spectra

In most cases, nonlinear effects have been observed experimentally on the lower polariton branch. So, neglecting the coupling of the two polariton branches by the exciton–exciton interaction term, equations (12) and (13) can be used to write the equation for the lower polariton (the lower branch index has been suppressed for simplicity):

$$\frac{d\hat{p}}{dt} = -(\gamma_p + i\delta_p)\hat{p} - 2i\alpha_p\hat{p}^\dagger\hat{p}\hat{p} - C_0\sqrt{2\gamma_a}\hat{a}^{\text{in}} + X_0\sqrt{2\gamma_b}\hat{b}^{\text{in}} \quad (27)$$

where $\alpha_p = X_0^4\alpha$, $\gamma_p = C_0^2\gamma_a + X_0^2\gamma_b$, $\delta_p = E_p/\hbar - \omega_L$.

Since electromagnetic, exciton and polariton fields have large average values compared with the fluctuations, equation (27) can be linearized for the small fluctuations. One sets:

$$\hat{a}(t) = a_0 + \delta\hat{a}(t), \quad \hat{b}(t) = b_0 + \delta\hat{b}(t), \quad \hat{p}(t) = p_0 + \delta\hat{p}(t) \quad (28)$$

where a_0 , b_0 and p_0 are the classical mean values derived in the previous section and $\delta\hat{a}(t)$, $\delta\hat{b}(t)$ and $\delta\hat{p}(t)$ are the quantum fluctuations of the field inside the cavity.

The Fourier transforms of the fluctuations of any operator $\delta\hat{o}(\omega)$ are defined as:

$$\delta\hat{o}(\omega) = \int \delta\hat{o}(t) e^{i\omega t} dt, \quad \delta\hat{o}^\dagger(\omega) = \int \delta\hat{o}^\dagger(t) e^{i\omega t} dt \quad (29)$$

where ω is a noise frequency. The frequencies ω over which the fields and their fluctuations vary appreciably are of the order of the relaxation rates and of the exciton–photon coupling rate g , that are much smaller than the optical frequency ω_L . Equation (27) and its Hermitian conjugate are linearized and Fourier transformed. This allows us to replace differential equations by linear algebraic equations:

$$\begin{aligned} -i\omega\delta\hat{p}(\omega) = & -(\gamma_p + i\delta_p)\delta\hat{p}(\omega) - 2i\alpha_p I_p \delta\hat{p}(\omega) - 2i\alpha_p p_0^2 \delta\hat{p}^\dagger(\omega) - C_0\sqrt{2\gamma_a}\delta\hat{a}^{\text{in}}(\omega) \\ & + X_0\sqrt{2\gamma_b}\delta\hat{b}^{\text{in}}(\omega) \end{aligned} \quad (30)$$

The presence of a term proportional to $\delta\hat{p}^\dagger$ on the right-hand side of this equation indicates that the system will behave as a parametric amplifier for fluctuations, amplifying some quadratures and de-amplifying other ones.

Solving this equation and its Hermitian conjugate yields the polariton fluctuation as a function of the incoming fluctuations. The fluctuations of the reflected field are easily deduced from equations (5) and (14). The squeezing spectra, that can be measured in the outgoing light with a radio-frequency spectrum analyser connected to photodetectors, are directly related to the quantities $\delta\hat{a}^{\text{out}}(\omega)$ and $\delta\hat{a}^{\text{out}\dagger}(\omega)$. Indeed, experiments allow us to measure the fluctuations of the output electric field in a quadrature defined by an angle θ with respect to some phase reference:

$$\delta\hat{x}_\theta^{\text{out}}(\omega) = e^{-i\theta}\delta\hat{a}^{\text{out}}(\omega) + e^{i\theta}\delta\hat{a}^{\text{out}\dagger}(\omega) \quad (31)$$

and the measured spectra are given by:

$$\delta\hat{x}_\theta^{\text{out}}(\omega)\delta\hat{x}_\theta^{\text{out}}(\omega') = 2\pi\delta(\omega + \omega')S_\theta(\omega) \quad (32)$$

The spectra of the outgoing fluctuations can thus be computed from the spectra of the incoming fluctuations given by equations (15) and (16). For any given cavity–exciton detuning, the spectra can be calculated either for a fixed laser detuning as a function of the fluctuation frequency ω , or for a fixed value of ω as a function of the laser detuning. The second case being better suited to the experimental conditions, the calculated spectra will be shown for $\omega = 0$ as a function of the laser detuning. Spectra are shown in two cases: ‘optimum’ squeezing spectra, for which θ is adjusted at each point in such a way that it gives the minimal amount of noise and intensity squeezing spectra for which the quantum fluctuations are calculated for the amplitude quadrature of the output field. The noise can be calculated for the upper branch in a similar way.

Fig. 1 shows a set of optimum squeezing spectra (left) and intensity squeezing spectra (right) at $\omega = 0$, as a function of the laser frequency δ , for cavity–exciton resonance ($\delta_a = \delta_b$), and three different situations corresponding to increasing temperatures: (a) at zero temperature, $\langle n \rangle = 0$, (b) $\langle n \rangle = 0.2$, (c) $\langle n \rangle = 1$. It can be seen that a squeezing of about 40% is predicted in the absence of phonon scattering, even with the low values of the non-linearity that have been assumed. Squeezing is observable on the intensity, even though it is lower than the optimum squeezing. Excess noise observed on the intensity is the counterpart of squeezing: quantum fluctuations can only be reduced in some quadrature if they are increased in another quadrature. In the presence of small phonon interactions squeezing can still be observed, but tends to disappear rapidly as $\langle n \rangle$ increases. The coupling to a thermal bath brings additional fluctuations into the system that appear as excess noise on the output field. This excess noise is detrimental to the observation of quantum effects. However, it is expected that the study of this noise can bring interesting information on the relaxation processes in the semiconductor microcavity.

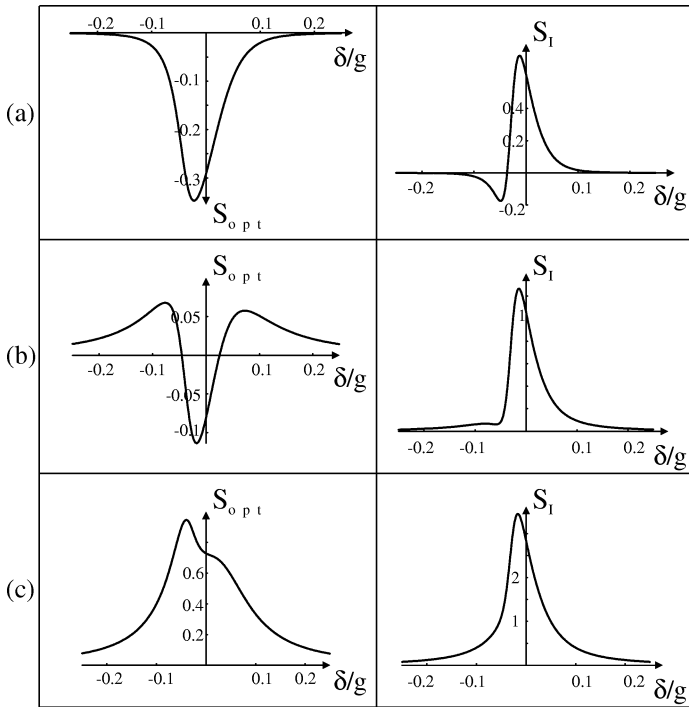


Figure 1. Optimum squeezing S_{opt} and intensity squeezing S_I (calculated at zero noise frequency) as a function of the laser detuning δ_p (normalized to g), when the cavity is resonant with the exciton for $\gamma_a = \gamma_b = 0.05g$, $2\alpha = 1.5 \cdot 10^5$ Hz, $I^{\text{in}} = 0.5I_0$, where I_0 is the incoming intensity yielding an exciton density of $10^9/\text{cm}^2$. The standard quantum noise corresponds to $S = 0$, perfect squeezing corresponds to $S = -1$. Curves (a), (b) and (c) correspond respectively to mean thermal excitation numbers $\langle n \rangle = 0, 0.2$ and 1 .

Quantum effects should then be observed in semiconductor microcavities at low temperature or in a system decoupled from the phonons. The decoupling of the lower polariton branch from relaxation has been predicted [35,37] and observed in recent experiments [36] and gives good prospect to such experiments.

5. Experiments

High finesse GaAs/AlAs microcavity samples containing either one or two InGaAs quantum wells with low indium content have been used [16,39]. These high-quality samples exhibit very narrow polariton linewidth, of the order of 100–200 μeV (half-width at half-maximum) at 4 K. The microcavities are wedged, allowing one to change the cavity thickness by moving the laser excitation spot on the samples. The beam of a single mode CW Ti:sapphire laser with a linewidth of the order of 1 MHz is focused onto the sample at normal incidence. The laser light is circularly polarized. The laser spot has a diameter of 80 μm .

First the positions of the two polariton branches are determined by studying the reflection of the driving laser at very low intensity ($I \lesssim 0.1 \text{ mW}$, corresponding to 1 W/cm^2), yielding the diagram shown in Fig. 3, where the energies of the reflectivity minima have been plotted as a function of their positions on the sample.

The light emitted by the microcavity is detected in the direction normal to the sample by means of a homodyne detection system [40,41]. For this purpose the emitted light is mixed with a local oscillator on a beamsplitter (Fig. 2). The emitted light of interest copropagates with the laser beam and has the same very small divergence angle ($\simeq 0.4^\circ$), ensuring the k_{\parallel} conservation. An additional laser beam, the local oscillator, is mixed with the pump and signal beam on a beamsplitter. The beams coming from the beamsplitter are focused on two photodetectors. The frequency spectrum of the photocurrents is analyzed with an RF spectrum analyzer. The reflected laser and the light scattered at the laser frequency yield a large peak at zero frequency which is filtered out. The signal given by the spectrum analyzer can be shown [41] to be proportional to the beat signal between the local oscillator and the light fluctuations emitted by the sample, that form incoherent luminescence. For this incoherent emission, the spectrum analyzer measures a broad signal, that appears on top of the background quantum noise (shot noise).

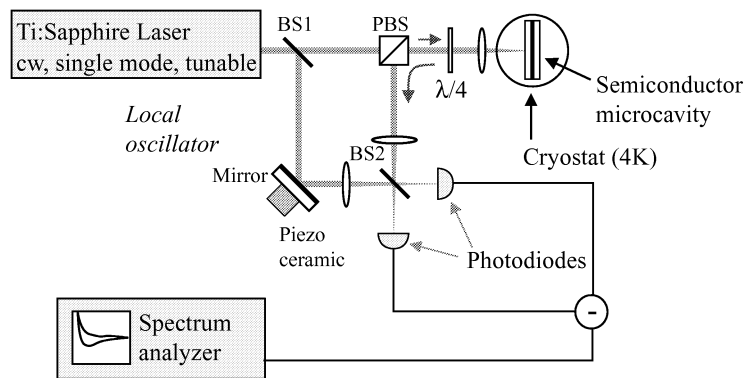


Figure 2. Experimental set-up. It can be used in two different configurations. (a) Without beamsplitter (BS1): the polarizing beamsplitter (PBS) and the quarter wave plate ($\lambda/4$) form an optical circulator that direct all the circularly polarized light coming from the microcavity towards the detection system. The 50/50 beamsplitter (BS) splits the beam into two equal parts which fall on two photodetectors. The sum of the two photocurrents gives the beat signal between the emission and the laser. The difference between the photodiode currents yields the shot noise. (b) With beamsplitter (BS1): an independent local oscillator is split off by the beamsplitter (BS1) and mixed with the beam emerging from the microcavity on (BS2). In this case, the beat signal between the emitted light and the local oscillator is obtained by taking the difference between the two photocurrents. The shot noise background is measured by blocking the beam emerging from the cavity.

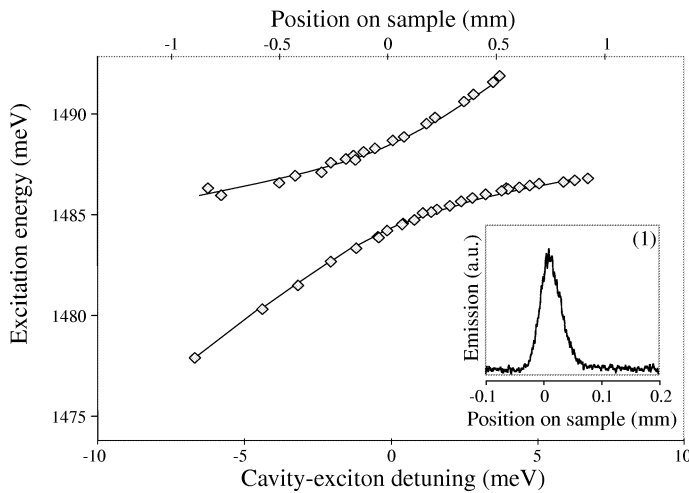


Figure 3. Energy diagram of the polariton branches as a function of position on the sample. Inset: emission resonance obtained when the laser position is scanned around zero detuning with fixed pump laser wavelength and $I_P = 0.7$ mW. Here and in the following figures, the analysis frequency of the spectrum analyzer is fixed at 7 MHz.

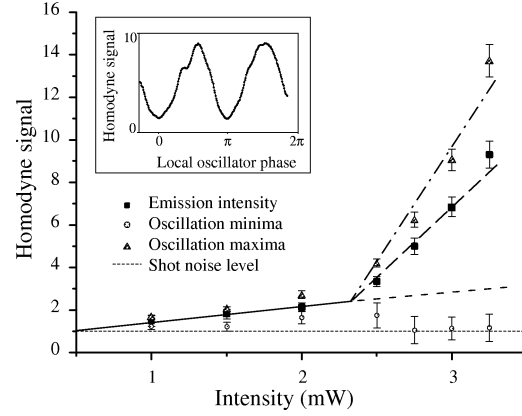
One of the mirrors on the path of the local oscillator is mounted on a piezoceramic, which allows one to vary its phase relative to the signal beam. This provides a tool to explore all the quadrature components for the emitted light. In some experiments, the local oscillator is simply the laser beam reflected by the microcavity, the beam splitter BS1 in Fig. 2 being suppressed. The phase difference between the detected signal and the local oscillator is fixed, since the emitted light and the reflected laser follow exactly the same path. This scheme allows measurement of the emission intensity that is in phase with the pump laser. Without homodyne detection, the emitted light would be extremely difficult to distinguish from the scattered and reflected laser light.

In order to study the noise emission resonances, a specific scanning method was used. The possible frequency scan of the detection system on each side of the laser line is of the order of a few tens of MHz, that is in the 100 neV range, much smaller than a typical photoluminescence spectrum. To investigate the emission, the frequency of the spectrum analyzer is kept fixed, while either the laser frequency or the position on the sample is scanned. Therefore, the detected polaritons have an energy extremely close to the ones excited by the pump laser. The emission lineshape obtained with the homodyne detection can be studied in the vicinity of the polariton resonance branches either by scanning the laser energy (“vertical” scan in Fig. 3) for fixed positions on the sample or by scanning the position of the laser on the sample (“horizontal” scan in Fig. 3) at fixed laser frequencies. Since it is difficult to scan a single mode laser continuously over ranges that are of the order of the polariton linewidth, the second procedure was chosen. The position scan amounts to varying the detuning between the polariton and the laser at a fixed laser frequency. An example of such a signal is shown in the inset of Fig. 3 for very low laser intensity.

When the pump laser intensity is high enough the noise is expected to be phase-dependent. Using homodyne detection allows one to explore this property. As in the experiment performed in reference [16], thermally excited polaritons constitute the probe that seeds the parametric process coming from equation (30) and that is amplified through interaction with the pumped polaritons. Having no average phase, the former can be considered as a superposition of random polariton fields with equal mean amplitudes and phases spread over 2π . For each value of the local oscillator phase, the emission having a specific phase is singled out by the homodyne detection. Scanning the local oscillator phase allows one to identify whether some quadrature components are amplified in a preferential way.

At low pump intensity, all quadrature components are equivalent. Starting a little below some threshold value, one observes an oscillation of the homodyne signal as a function of the local oscillator phase. A typical recording is shown in Fig. 4 (inset), at zero-cavity–exciton detuning. The threshold takes place at very low excitation intensities. It is as low as 2 mW of incident laser power over a spot of 80 μm in diameter

Figure 4. Amplitude of the minima and maxima of the oscillations as a function of the driving laser intensity; the driving laser frequency is fixed and equal to the unshifted (i.e. measured at very low intensity) lower polariton frequency at zero detuning; the position on sample is adjusted to maximize the emission intensity on the lower branch. Dash-dotted and dashed lines: guides to the eye respectively for the oscillation maxima and the emission intensity above threshold. Solid line: thermal emission intensity below threshold. Dotted line: extrapolated thermal emission. Inset: homodyne detection signal (arbitrary units) when the phase of the local oscillator is varied for zero exciton laser detuning on the lower branch of sample 1. The driving laser power is 3 mW. The oscillation period is π rather than 2π because the probe is constituted by an ensemble of random fields in which phases φ and $\varphi + \pi$ are equivalent.



(20 W/cm²). The threshold is lowest for values of the cavity–exciton detuning close to zero. All the considered pump intensities correspond to exciton densities that are below the polariton bleaching density. This was verified by checking the presence of vacuum Rabi splitting in reflectivity for these intensities. No non-linear emission was observed on the upper polariton branch in the same range of laser powers. This clearly demonstrates the phase dependence of the polariton field typical of degenerate parametric amplification [38]. The evolution equation (30) for the generated polariton fluctuations $\delta\hat{p}$ contains a gain term proportional to $2i\alpha_p p_0^2 \delta\hat{p}^\dagger$ coming from polariton four-wave mixing. This term implies a well-defined phase relationship between the pump field and the amplified polariton quadrature. An amplification originating from population effects, as in a laser, would be phase independent.

The amplitude of the oscillation grows rapidly with the pump field intensity above threshold. In Fig. 4, the maxima and minima of the oscillations are shown as a function of the driving laser power, obtained at fixed laser frequency and by shifting the sample in order to compensate for the energy shift due to the term $2i\alpha_p I_p \delta\hat{p}(\omega)$ in equation (30) and also derived by other authors [13]. The level of thermal luminescence in the absence of nonlinear process, extrapolated from its value below threshold is also shown. It can be seen that the oscillation minimum goes well below the level of thermal luminescence, indicating a strong deamplification of thermal polaritons. This effect is a specific feature of parametric interaction. If deamplification is efficient enough, squeezing of the emission below the shot noise level could be achieved. Deamplification down to the shot noise level, i.e. to the vacuum noise is obtained here. The quadrature component of the emitted field along the mean field of the pump laser, which can be called emission intensity, that is measured using the first experimental scheme, undergoes intermediate amplification.

In conclusion, a quantum theory of the polariton field in semiconductor microcavities shows that quantum effects are predicted to originate from coherent polariton–polariton interaction. Using homodyne detection, evidence for specific features of polariton four-wave mixing in the microcavity was obtained. The phase dependence of the amplification process and the occurrence of deamplification demonstrate the coherent origin of the process. Since in such nonlinear interactions amplification and squeezing originate from the same physical effect, this opens the way to the possibility of squeezing in semiconductor microcavity devices. Quantum properties should also be observed when the cavity is pumped at the ‘magic’ angle. In such a case, a behaviour similar to the one of an optical parametric oscillator is expected, with quantum correlations between the signal and idler fields.

References

- [1] C. Weisbuch et al., Phys. Rev. Lett. 69 (1992) 3314–3317;
R. Houdré et al., Phys. Rev. Lett. 73 (1994) 2043–2046.
- [2] J. Rarity, in: C. Weisbuch (Ed.), *Microcavities and Photonic Bandgaps*, Kluwer, 1996.
- [3] S. Haroche, Cavity quantum electrodynamics, in: *Fundamental Systems in Quantum Optics*, Elsevier, 1992, p. 768;
G. Rempe, R.J. Thompson, R.J. Brecha, W.D. Lee, H.J. Kimble, Phys. Rev. Lett. 67 (1991) 1727.
- [4] S.W. Koch, N. Peygambarian, M. Lindberg, J. Phys. C 21 (1988) 5229.
- [5] A. Mysyrowicz, D. Hulin, A. Antonetti, A. Migus, W.T. Masselink, H. Morkoc, Phys. Rev. Lett. 55 (1986).
- [6] A.M. Fox, J.J. Baumberg, M. Dabbicco, B. Huttner, J.F. Ryan, Phys. Rev. Lett. 74 (1995) 1728.
- [7] E. Hanamura, in: J. Rarity, C. Weisbuch (Eds.), *Microcavities and Photonic Bandgaps*, Kluwer, 1996.
- [8] V. Savona, Z. Hradil, A. Quattropani, Phys. Rev. B 49 (1994) 8774.
- [9] S. Savasta, R. Girlanda, Phys. Rev. Lett. 77 (1996) 4736.
- [10] H. Eleuch, J.M. Courty, G. Messin, C. Fabre, E. Giacobino, J. Opt. B 1 (1999) 1.
- [11] G. Messin, J.Ph. Karr, H. Eleuch, J.M. Courty, E. Giacobino, J. Phys. Cond. Matter 11 (1999) 6069.
- [12] E. Hanamura, J. Phys. Soc. Japan 37 (1974) 1545;
J. Phys. Soc. Japan 37 (1974) 1553.
- [13] C. Ciuti, P. Schwendimann, B. Devaud, A. Quattropani, Phys. Rev. B 62 (2000) R4825.
- [14] P.G. Savvidis, J.J. Baumberg, R.M. Stevenson, M.S. Skolnick, D.M. Whittaker, J.S. Roberts, Phys. Rev. Lett. 84 (2000) 1547.
- [15] R. Huang, F. Tassone, Y. Yamamoto, Phys. Rev. B 61 (2000) R7854.
- [16] R. Houdré, C. Weisbuch, R.P. Stanley, U. Oesterle, M. Ilegems, Phys. Rev. Lett. 85 (2000) 2793.
- [17] R.M. Stevenson, V.N. Astranov, M.S. Skolnick, D.M. Whittaker, M. Emam-Ismaïl, A.I. Tartakovskii, P.G. Savvidis, J.J. Baumberg, J.S. Roberts, Phys. Rev. Lett. 85 (2000) 3680.
- [18] G. Messin, J.Ph. Karr, A. Baas, G. Khitrova, R. Houdré, R.P. Stanley, U. Oesterle, E. Giacobino, Phys. Rev. Lett. 87 (2001) 127403.
- [19] H. Haug, Z. Phys. B 24 (1976) 351.
- [20] Ba An Nguyen, Phys. Rev. B 48 (1993) 11732.
- [21] W.H. Louisell, *Quantum Statistical Properties of Radiation*, Wiley, New York, 1973.
- [22] M.L. Steyn-Ross, C.W. Gardiner, Phys. Rev. A 27 (1983) 310.
- [23] C. Cohen-Tannoudji, J. Dupont-Roc, G. Grynberg, *Processus d'interaction entre photons et atomes*, InterÉditions/Éditions du CNRS, Paris, 1988, p. 309.
- [24] C. Piermarocchi, F. Tassone, V. Savona, A. Quattropani, P. Schwendimann, Phys. Rev. B 53 (15) (1996) 584.
- [25] F. Tassone, C. Piermarocchi, V. Savona, A. Quattropani, P. Schwendimann, Phys. Rev. B 53 (1996) R7642;
F. Tassone, C. Piermarocchi, V. Savona, A. Quattropani, P. Schwendimann, Phys. Rev. B 56 (1997) 7554.
- [26] C. Ciuti, V. Savona, C. Piermarocchi, A. Quattropani, P. Schwendimann, Phys. Rev. B 58 (1998) 7926.
- [27] J.Ph. Karr, Thèse, Paris, 2001.
- [28] H. Eleuch, Thèse, Paris, 1998.
- [29] L.A. Orozco, M.G. Raizen, Min Xiao, R.J. Brecha, H.J. Kimble, J. Opt. Soc. Am. B 4 (1987) 1490;
H.J. Carmichael, Phys. Rev. A 33 (1986) 3262.
- [30] M.J. Collett, C.W. Gardiner, Phys. Rev. A 30 (1984) 1386;
S. Reynaud, A. Heidmann, Opt. Commun. 71 (1989) 209;
S. Reynaud, C. Fabre, E. Giacobino, A. Heidmann, Phys. Rev. A 40 (1989) 1440.
- [31] Y. Toyozawa, Prog. Theor. Phys. 20 (1958) 53.
- [32] B. Sermage, S. Long, I. Abram, J.Y. Marzin, J. Bloch, R. Planel, V. Thierry-Mieg, Phys. Rev. B 53 (1996) 16516.
- [33] R. Houdré, J.L. Gibernon, P. Pellandini, R.P. Stanley, U. Oesterle, C. Weisbuch, J. O'Gorman, B. Roycroft, M. Ilegems, Phys. Rev. B 52 (1995) 7810.
- [34] T.R. Nelson, E.K. Lindmark, D.V. Vick, K. Tai, G. Khitrova, H.M. Gibbs, in: J. Rarity, C. Weisbuch (Eds.), *Microcavities and Photonic Bandgaps*, Kluwer, 1996.
- [35] C. Ciuti, V. Savona, C. Piermarocchi, A. Quattropani, P. Schwendimann, Phys. Rev. B 58 (1998) R10123.
- [36] X. Marie, P. Renucci, S. Dubourg, T. Amand, P. Le Jeune, J. Bloch, R. Planel, Phys. Rev. B 59 (1999) R2494.
- [37] F. Tassone, Y. Yamamoto, Phys. Rev. B 59 (1999) 10830.
- [38] A. Yariv, *Quantum Electronics*, 3rd edition, Wiley, New York, 1989, Chapter 17.
- [39] J. Rarity, C. Weisbuch (Eds.), *Microcavities and Photonic Bandgaps*, Kluwer, 1996, pp. 43–57.
- [40] Y. Yamamoto, T. Kimura, IEEE J. Quantum Electron. QE-17 (1981);
H. van de Stadt, Astron. Astrophys. 36 (1974) 341.
- [41] H.P. Yuen, V.W.S. Chan, Opt. Lett. 8 (1983) 177.